Spherically symmetric models of scalar field's interaction

Victor L. Mironov, Sergey V. Mironov

Institute for physics of microstructures RAS, GSP-105, Nizhny Novgorod, 603950, Russia

E-mail: mironov@ipmras.ru

Abstract

We discuss the particles and fields described by a hypercomplex first-order wave equation with nonzero mass of quantum. It is shown that the strengths of such fields are nonzero only in the area of sources. This allows us to consider scalar particles as localized regions of space filled with a scalar field. The interaction of such regions occurs only when they overlap. First, we consider simple spherically symmetric models of scalar particles in the form of homogeneous spherical regions filled with a scalar field and show that the spheres overlap leads to purely attractive or repulsive interactions. Then we generalize our results to more complex models of core-shell systems and demonstrate the formation of non-monotonic attractive/repulsive potential that provide metastable bound states and annihilation barriers.

1. Introduction

Over the past two decades, significant progress has been achieved in describing fields with zero and nonzero mass of quantum based on hypercomplex wave equations [1-15]. In particular, factorization of the Klein-Gordon operator on the basis of various noncommutative hypercomplex algebras made it possible to formulate a second-order wave equation for the potentials of the field with non-zero mass of quantum, which is equivalent to the system of first-order equations for field strengths similar to the system of Maxwell equations [9-17]. Such approach allows us to apply the analogy of the classical electrodynamics formalism for the description of massive fields. At the same time, the essential difference in this case is that in the equations, along with vector fields, scalar fields are appeared, which are described by scalar field strengths [17]. This opens up new possibilities for the development of alternative models for the interaction of physical objects. In the present paper, we use this approach to construct models for the interaction of spherically symmetric sources of scalar fields.

2. Theoretical background

2.1. Space-time algebra

For compact writing of equations, we use the hypercomlex space-time algebra based on Macfarlane quaternions [18]. In this algebra any vector is presented in the basis of unit vectors $\mathbf{a}_1$, $\mathbf{a}_2$, $\mathbf{a}_3$ as

$$A = A_1\mathbf{a}_1 + A_2\mathbf{a}_2 + A_3\mathbf{a}_3, \tag{1}$$

with the following rules of multiplication and commutation:

$$\mathbf{a}_n\mathbf{a}_m = \delta_{nm} + i\lambda_{nmk}\mathbf{a}_k, \tag{2}$$

where δ_{nm} is Kronecker delta, λ_{nmk} is Levi-Civita symbol ($n,m,k \in \{1,2,3\}$) and i is the imaginary unit ($i^2 = -1$). The main advantage of this algebra is the Clifford product of vectors, which is represented as the sum of scalar and vector products

$$AB = (A \cdot B) + i[A \times B]. \tag{3}$$

This allows writing the equations in a very compact form. To compactify the operator parts of equations we use additional units $\mathbf{e}_1, \mathbf{e}_2, \mathbf{e}_3$ with the same rules of multiplication

$$\mathbf{e}_n \mathbf{e}_m = \delta_{nm} + i\lambda_{nmk}\mathbf{e}_k. \tag{4}$$

The basis $\mathbf{a}_1, \mathbf{a}_2, \mathbf{a}_3$ is associated with spatial rotation of vector values, while basis $\mathbf{e}_1, \mathbf{e}_2, \mathbf{e}_3$ connected with space-time inversion [19]. The unit vectors $\mathbf{a}_n$ commute with units $\mathbf{e}_m$

$$\mathbf{a}_n \mathbf{e}_m = \mathbf{e}_m \mathbf{a}_n. \tag{5}$$

Further we use this formalism to describe the fields with nonzero mass of quantum.

2.2. The equations for the fields with nonzero mass of quantum

The hypercomplex wave equation for a field with nonzero mass of quantum is written in the following form [17,19]:

$$\left(i\mathbf{e}_1 \frac{1}{c}\frac{\partial}{\partial t} - \mathbf{e}_2 \nabla - i\mathbf{e}_3 m \right)\left(i\mathbf{e}_1 \frac{1}{c}\frac{\partial}{\partial t} - \mathbf{e}_2 \nabla - i\mathbf{e}_3 m \right)\tilde{\mathbf{W}} = \tilde{\mathbf{J}}, \tag{6}$$

where parameter $m = m_0 c / \hbar$ (m_0 is mass of quantum, c is the speed of light, $\hbar$ is Plank's constant).

The quaternion field potential $\tilde{\mathbf{W}}$ is expressed in terms of the scalar $\varphi(r,t)$ and vector $\mathbf{A}(r,t)$ potentials

$$\tilde{\mathbf{W}} = i\mathbf{e}_1 \varphi + \mathbf{e}_2 \mathbf{A}. \tag{7}$$

The quaternion field source is

$$\tilde{\mathbf{J}} = -i\mathbf{e}_1 4\pi \rho_B + \mathbf{e}_2 \frac{4\pi}{c} j_B, \tag{8}$$

where ρ_B is the volume density of charge and j_B is the volume density of current. Introducing the scalar and vector field strengths

$$\begin{aligned}
g &= -m\varphi, \\
E &= -\frac{1}{c}\frac{\partial \mathbf{A}}{\partial t} - \nabla \varphi, \\
H &= [\nabla \times \mathbf{A}], \\
G &= -m\mathbf{A},
\end{aligned} \tag{9}$$

and taking into account the Lorentz gauge

$$\frac{1}{c}\frac{\partial \varphi}{\partial t} + (\nabla \cdot \mathbf{A}) = 0, \tag{10}$$

we rewrite the wave equation (6) in the following form:

$$\left(i\mathbf{e}_1 \frac{1}{c}\frac{\partial}{\partial t} - \mathbf{e}_2 \nabla - i\mathbf{e}_3 m \right)\left(i\mathbf{e}_2 g - i\mathbf{H} + \mathbf{e}_1 G + \mathbf{e}_3 E \right) = 0. \tag{11}$$

This hypercomplex equation is equivalent to the following system of Maxwell-like equations for field strengths:

$$\frac{1}{c}\frac{\partial g}{\partial t}+\left(\nabla\cdot\boldsymbol{G}\right)=0,$$

$$\frac{1}{c}\frac{\partial\boldsymbol{G}}{\partial t}+\nabla g-m\boldsymbol{E}=0,$$

$$\frac{1}{c}\frac{\partial\boldsymbol{H}}{\partial t}+\left[\nabla\times\boldsymbol{E}\right]=0,$$

$$\frac{1}{c}\frac{\partial\boldsymbol{E}}{\partial t}-\left[\nabla\times\boldsymbol{H}\right]+m\boldsymbol{G}=-\frac{4\pi}{c}\boldsymbol{j}_B, \tag{12}$$

$$\left[\nabla\times\boldsymbol{G}\right]+m\boldsymbol{H}=0,$$

$$\left(\nabla\cdot\boldsymbol{E}\right)-mg=4\pi\rho_B,$$

$$\left(\nabla\cdot\boldsymbol{H}\right)=0.$$

Multiplying each of the equations of system (12) by the corresponding field strength and adding, we get:

$$\frac{1}{2c}\frac{\partial}{\partial t}\left(g^2+\boldsymbol{E}^2+\boldsymbol{H}^2+\boldsymbol{G}^2\right)+\left(\boldsymbol{E}\cdot\left[\nabla\times\boldsymbol{H}\right]\right)-\left(\boldsymbol{H}\cdot\left[\nabla\times\boldsymbol{E}\right]\right)+g\left(\nabla\cdot\boldsymbol{G}\right)+\left(\boldsymbol{G}\cdot\nabla g\right)+4\pi\left(\boldsymbol{E}\cdot\boldsymbol{j}_B\right)=0. \tag{13}$$

Denote

$$w=\frac{1}{8\pi}\left(g^2+\boldsymbol{E}^2+\boldsymbol{H}^2+\boldsymbol{G}^2\right),$$

$$\boldsymbol{P}=\frac{c}{4\pi}\left(g\boldsymbol{G}+\left[\boldsymbol{E}\times\boldsymbol{H}\right]\right). \tag{14}$$

Then expression (13) can be represented as

$$\frac{\partial w}{\partial t}+\left(\nabla\cdot\boldsymbol{P}\right)+\left(\boldsymbol{E}\cdot\boldsymbol{j}_B\right)=0. \tag{15}$$

This is an analogue of Poynting's theorem for fields with non-zero mass of quantum. In this case, the value w plays the role of the volume density of energy and $\boldsymbol{P}$ is the vector of energy flux.

2.3. Inhomogeneous first-order wave equation

Let us consider a special class of fields described by a hypercomplex first-order wave equation [17,19]:

$$\left(i\mathbf{e}_1\partial-\mathbf{e}_2\nabla-i\mathbf{e}_3m\right)\tilde{\mathbf{W}}=\tilde{\mathbf{I}}. \tag{16}$$

The field potential $\tilde{\mathbf{W}}$ is

$$\tilde{\mathbf{W}}=i\mathbf{e}_1\varphi+\mathbf{e}_2\boldsymbol{A}. \tag{17}$$

The source $\tilde{\mathbf{I}}$ is represented as

$$\tilde{\mathbf{I}}=-i\mathbf{e}_2 4\pi\rho_L+\mathbf{e}_1\frac{4\pi}{c}\boldsymbol{j}_L, \tag{18}$$

where ρ_L is the volume density of charge and $\boldsymbol{j}_L$ is the volume density of current. Taking into account definitions (9), the equation (16) reduces to the equation for field strengths:

$$-i\mathbf{e}_2 g+\mathbf{e}_1\boldsymbol{G}=-i\mathbf{e}_2 4\pi\rho_L+\mathbf{e}_1\frac{4\pi}{c}\boldsymbol{j}_L, \tag{19}$$

which is equivalent to the following system:

$$g=4\pi\rho_L,$$

$$\boldsymbol{G}=\frac{4\pi}{c}\boldsymbol{j}_L. \tag{20}$$

These equations mean that the field strengths are nonzero only in the region of sources.

In the stationary case, the current j_L is zero and the system is completely described by a scalar field g. This allows us to interpret the particles described by equation (16) as localized regions of space filled with scalar field g. The energy of a system consisting of two regions filled with scalar fields g_1 and g_2 is equal to

$$W = \frac{1}{8\pi} \int_V (g_1 + g_2)^2 dV = W_1 + W_2 + W_{12},$$ (21)

where W_1 is energy of first region, W_2 is energy of the second region, W_{12} is the energy of interaction between regions. The interaction energy is

$$W_{12} = \frac{1}{4\pi} \int_V g_1 g_2 \, dV.$$ (22)

This value is nonzero only in the case when the regions have an overlap in space. Further we consider various models of particles in the form of spherical regions filled with a scalar field g.

3. Spherical models of scalar particles

3.1. Spherical particles with equal diameters

Let us consider a system of two identical particles in the form of spherical regions of radius R filled with a scalar field g (Fig. 1a).
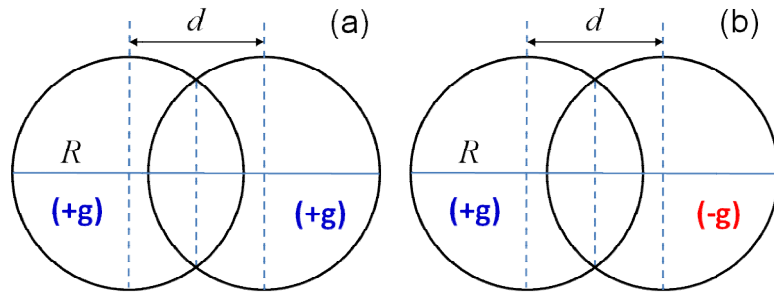

Fig. 1. The overlap of two spherical regions with scalar field g. (a) The system of particle-particle. (b) The system of particle-antiparticle.

Following (22) we find the dependence of the interaction energy in this system on the distance between the centers of the spheres. In this case, the problem is reduced to finding the volume of the area of intersection between two spheres, which is equal to

$$V_{sec} = \frac{2\pi}{3} \left(R - \frac{d}{2}\right)^2 \left(3R - \left(R - \frac{d}{2}\right)\right)$$ (23)

where d is the distance between the centers of the spheres. Accordingly, the interaction energy is

$$W_{12} = \frac{1}{4\pi} g^2 V_{sec} = \frac{1}{6} g^2 \left(R - \frac{d}{2}\right)^2 \left(3R - \left(R - \frac{d}{2}\right)\right)$$ (24)

Denote $x = d/R$ ($x \in \{0 \div 2\}$) and normalize W_{12} to the energy equal to the energy of two non-overlapping regions $2W_1 = \frac{1}{3} g^2 R^3$. Then we have following expression for the normalized interaction energy

4

$$\tilde{W}_{12} = \frac{1}{2}\left(1 - \frac{x}{2}\right)^2\left(3 - \left(1 - \frac{x}{2}\right)\right). \tag{25}$$

The dependence of $\tilde{W}_{12}$ on the overlap of two spheres characterizing purely repulsive interaction is shown in Fig. 2.
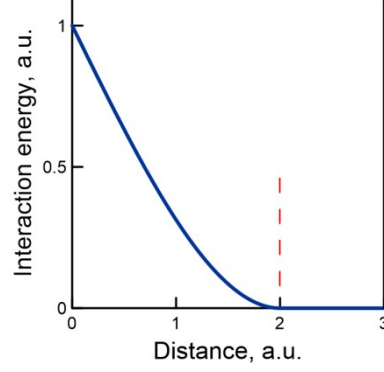

Fig. 2. Dependence of the interaction energy of two identical spherical particles (Fig. 1a) on the distance between the centers. The vertical dotted line shows the point of contact between the spheres.

Figure 2 shows that regions with identical fields repel each other. The repulsive force is

$$F_{12} = -\frac{1}{6}g^2\left(R - \frac{d}{2}\right)\left(\frac{3}{2}\left(R - \frac{d}{2}\right) - 3R\right). \tag{26}$$

It reaches the maximum at $d = 0$

$$F_{12} = \frac{1}{4}g^2R^2. \tag{27}$$

If the scalar fields have a different signs (Fig. 1b), then the annihilation of the particle and antiparticle at the overlap is realized. In this case, the total energy of the system becomes equal to zero. The corresponding dependence of the interaction energy $\tilde{W}_{12}$ on the degree of overlapping is shown in Fig. 3.
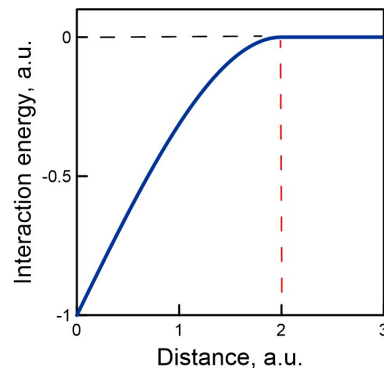

Fig. 3. Dependence of the interaction energy of two spherical particles with scalar fields of the opposite sign (Fig. 1b) on the distance between the centers. The vertical dotted line shows the point of contact between the spheres.

5

3.2. Spherical particles of different diameters

If one of the particles has a radius greater than other ($R_1 > R_2$), then a small particle is absorbed. Figure 4 shows the overlap of particles with fields of the same magnitude but different in sign.
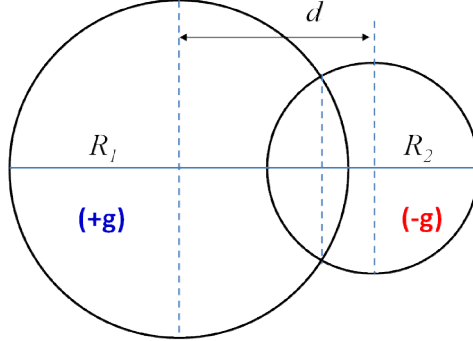

Fig. 4. The overlap of two particles with different diameters and different signs of the scalar field.

The volume of the overlapping spherical areas of different radii is equal to

$$V_{sec} = \frac{\pi}{12d}\left(R_1 + R_2 - d\right)^2\left(d^2 + 2d\left(R_1 + R_2\right) - 3\left(R_1 - R_2\right)^2\right). \tag{28}$$

Accordingly, the interaction energy is

$$W_{12} = -\frac{1}{48}\frac{g^2}{d}\left(R_1 + R_2 - d\right)^2\left(d^2 + 2d\left(R_1 + R_2\right) - 3\left(R_1 - R_2\right)^2\right). \tag{29}$$

We normalize W_{12} to value equal to the double energy of a small particle $2W_2 = \frac{1}{3}g^2R_2^3$ and denote $\lambda = \frac{R_1}{R_2}$, $y = \frac{d}{R_2}$. Then the normalized energy of interaction is equal to

$$\tilde{W}_{12} = -\frac{1}{16y}\left(\lambda + 1 - y\right)^2\left(y^2 + 2y\left(\lambda + 1\right) - 3\left(\lambda - 1\right)^2\right). \tag{30}$$

As an example, Fig. 5 shows the dependence of the interaction energy for the case $\lambda = 2$.
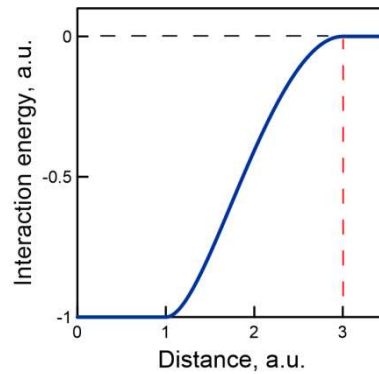

Fig. 5. Dependence of the interaction energy of two spherical particles ($\lambda = 2$) on the distance between the centers. The vertical dotted line shows the point of contact between the spheres.

3.3. Spherical core-shell particles

Let us consider two identical spherical core-shell particles (Fig. 6a) with core radius R_c and shell radius R_{sh}. The scalar field in the core is g_c and field in the shell is g_{sh}.
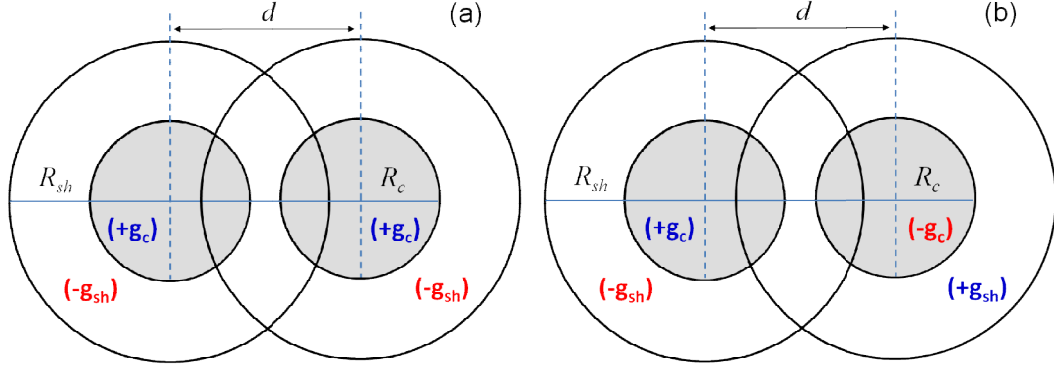

Fig. 6. The overlap of two spherical core-shell systems. (a) The system of particle-particle. (b) The system of particle-antiparticle.
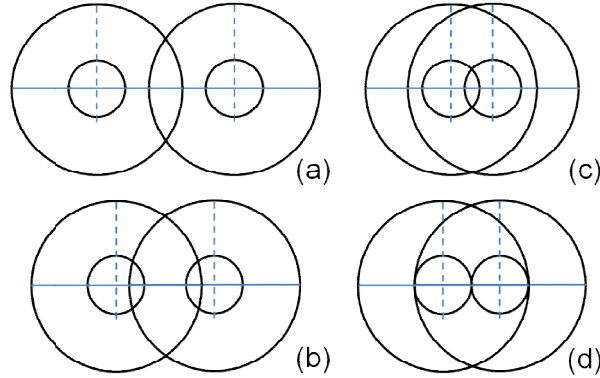

Fig. 7. The different phases of overlapping for two core-shell systems.

In this case, the calculation of the interaction energy is reduced to the calculation of the intersection volumes of spheres in situations corresponding to the three phases of overlapping shown in Fig. 7(a,b,c). In the first phase (Fig. 7a), the shell interaction energy is equal to

$$W_{12}^I = -\frac{1}{6}g_{sh}^2\left(R_{sh}-\frac{d}{2}\right)^2\left(3R_{sh}-\left(R_{sh}-\frac{d}{2}\right)\right). \tag{31}$$

Denote $\lambda = \dfrac{R_{sh}}{R_c}$, $\xi = \dfrac{g_c}{g_{sh}}$ and $z = \dfrac{d}{R_c}$. We normalize the energy W_{12}^I by a value $W = \dfrac{1}{3}g_{sh}^2 R_{sh}^3$, which is equal to double energy of a sphere with radius R_{sh} filled by the field g_{sh}. Then the normalized interaction energy of two core-shell particles in the first phase $z \in \{2\lambda \div (\lambda+1)\}$ (Fig. 7a) is expressed as follows:

$$\tilde{W}_{12}^{I} = \frac{1}{2\lambda^3}\left(\lambda - \frac{z}{2}\right)^2\left(3\lambda - \left(\lambda - \frac{z}{2}\right)\right). \tag{32}$$

The normalized interaction energy in the second phase $z \in \{(\lambda + 1) \div 2\}$ (Fig. 7b) is equal to

$$\tilde{W}_{12}^{II} = \frac{1}{2\lambda^3}\left(\lambda - \frac{z}{2}\right)^2\left(3\lambda - \left(\lambda - \frac{z}{2}\right)\right)$$
$$- \frac{(\xi + 1)}{8\lambda^3 z}(\lambda + 1 - z)^2\left(z^2 + 2z(\lambda + 1) - 3(\lambda - 1)^2\right). \tag{33}$$

The normalized interaction energy in the third phase (Fig. 7c) is

$$\tilde{W}_{12}^{III} = \frac{1}{2\lambda^3}\left(\lambda - \frac{z}{2}\right)^2\left(3\lambda - \left(\lambda - \frac{z}{2}\right)\right)$$
$$+ \frac{1}{2\lambda^3}\left(1 + 2\xi + \xi^2\right)\left(1 - \frac{z}{2}\right)^2\left(3 - \left(1 - \frac{z}{2}\right)\right) - \frac{2}{\lambda^3}(1 + \xi). \tag{34}$$

Let us consider the core-shell system with $R_{sh} = 3R_c$ ($\lambda = 3$). In this case, the shell of one system completely absorbs the core region of the other system (Fig. 7d). As an illustration, Fig. 8 demonstrates the dependences of interaction energy on the distance in cases $\xi = 1$ and $\xi = 10$.
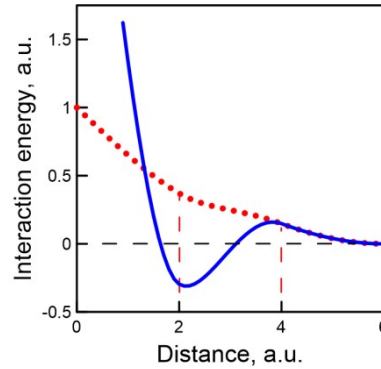

Fig. 8. Dependences of the interaction energy of two identical core-shell particles on the distance between cents. Dotted line is for the case $\xi = 1$, solid line is for $\xi = 10$. Vertical dashed lines show the points of contact of the spherical regions in accordance with the phases represented in Fig. 7.

In the case $g_c = g_{sh}$ ($\xi = 1$), the shell repulsion dominates in the interaction (see dotted curve in Fig. 8). If $g_c \gg g_{sh}$, then we have a minimum of the energy, which corresponds to the bound state of two systems provided by their attraction when the shells overlap with the cores (Fig. 7d). As an example, the interaction energy of two core-shell particles with parameter $\xi = 10$ is represented in Fig. 8 (solid curve). In this case, a stronger repulsion is realized with a complete overlap of particles, provided by interaction between the cores.

If core-shell particles differ in signs of shell and core fields (Fig. 6b), then such systems annihilate with full overlap. Figure 9 shows the graphs of the interaction energy for the case $\xi = 1$ (sharp curve) and for the case $\xi = 10$ (solid curve).
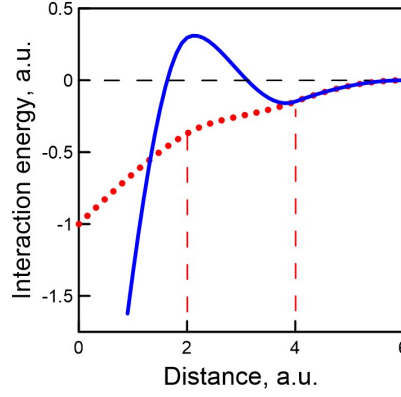
Fig. 9. Dependences of the interaction energy of two core-shell systems with fields of opposite sign on the distance between centers. Dotted line for case $\xi = 1$, solid line for case $\xi = 10$. Vertical dashed lines show the points of contact of the spherical regions in accordance with the phases represented in Fig. 7.

It can be seen from the figure that, in the case $g_c \gg g_{sh}$ ($\xi = 10$), an annihilation barrier appears due to repulsion between the shells and the cores (Fig. 7b).

4. Conclusion

Thus, we have considered several basic models of spherical particles interacting through the overlap of scalar fields. Depending on the signs of the fields, the particles are either repelled or attracted. The most interesting are the models of particles that have the core-shell structure. These models can be used to describe bound states in a system of two identical particles. In this case, the binding force is determined by the ratio of the fields in the shell and the core. On the other hand, the core-shell model provides a barrier to particle-antiparticle annihilation. The value of the annihilation barrier also depends on the ratio of the fields in the cores and shells. Potentially, the considered phenomenological approach can be used to model short-range interactions in baryon-baryon and baryon-lepton systems.

References

1. S. Demir, M. Tanişli, N. Candemir, Hyperbolic quaternion formulation of electromagnetism, Advances in Applied Clifford Algebras, **20**(3–4), 547–563 (2010).

2. V.L. Mironov, S.V. Mironov, Octonic representation of electromagnetic field equations, Journal of Mathematical Physics, **50**, 012901 (2009).

3. S. Demir, M. Tanişli, M.E. Kansu, Octonic massless field equations, International Journal of Modern Physics A, **30** (15), 1550084 (2015).

4. B.C. Chanyal, S.K. Chanyal, Ö. Bektaş, S. Yce, A new approach on electromagnetism with dual number coefficient octonion algebra, International Journal of Geometric Methods in Modern Physics, **13**(9), 1630013 (2016).

5. M.E. Kansu, Quaternionic representation of electromagnetism for material media, International Journal of Geometric Methods in Modern Physics, **16**(7), 1950105 (2019).

6. S. Giardino, Quaternionic electrodynamics, Modern Physics Letters A, **35**(39) 2050327 (2020).

7. Z.-H. Weng, Forces in the complex octonion curved space, International Journal of Geometric Methods in Modern Physics, **13**(6) 1650076 (2016).

8. İ. Aymaz, M.E. Kansu, Dual-complex quaternion representation of gravitoelectromagnetism, International Journal of Geometric Methods in Modern Physics, **18** (11), 2150178 (2021).

9. S. Ulrych, The Poincare mass operator in terms of a hyperbolic algebra, Physics Letters B, **612**(1-2), 89-91 (2005).

10. C. Cafaro, S.A. Ali, The spacetime algebra approach to massive classical electrodynamics with magnetic monopoles, Advances in Applied Clifford Algebras, **17**, 23-36 (2006).

11. N. Candemir, M. Tanişli, K. Özdas, S. Demir, Hyperbolic octonionic Proca-Maxwell equations, Zeitschrift für Naturforschung A, **63**(1-2), 15-18 (2008).

12. S. Ulrych, Considerations on the hyperbolic complex Klein-Gordon equation, Journal of Mathematical Physics, **51**(6), 063510 (2010).

13. S. Demir, M. Tanişli, A compact biquaternionic formulation of massive field equations in gravi-electromagnetism, European Physical Journal – Plus, **126**, 115 (2011).

14. S. Ulrych, Higher spin quaternion waves in the Klein-Gordon theory, International Journal of Theoretical Physics, **52**(1), 279-292 (2013).

15. Z.-H. Weng, Four interactions in the sedenion curved spaces, International Journal of Geometric Methods in Modern Physics, **16**(2) 1950019 (2019).

16. B.C. Chanyal, Generalized Klein-Gordon field equations with octonion space-time (OST) algebra, Chinese Journal of Physics, **55**(2), 432-443 (2017).

17. S.V. Mironov, V.L. Mironov, Sedeonic equations of massive fields, International Journal of Theoretical Physics, **54**(1), 153-168 (2015).

18. A. Macfarlane, Hyperbolic quaternions, Proceedings of the Royal Society at Edinburgh, 1899-1900 session, p. 169-181 (1900).

19. V.L. Mironov, S.V. Mironov, Sedeonic equations in field theory, Advances in Applied Clifford Algebras, **30**, 44 (2020).